frontiers | Frontiers in Earth Science

ORIGINAL RESEARCH
published: 14 April 2022
doi: 10.3389/feart.2022.857729

Characteristics of Lithofacies Combinations and Reservoir Property of Carbonate-Rich Shale in Dongying Depression, Eastern China

Huimin Liu[1], Shun Zhang[2], Yali Liu[2], Pengfei Zhang[2], Xiaoliang Wei[2], Yong Wang[2], Deyan Zhu[2], Qinhong Hu[3], Wanqin Yang[2], Dong Tang[2], Fangxing Ning[2], Li Guan[2] and Youshu Bao[2]*

[1]Sinopec Shengli Oilfield Company, Dongying, China, [2]Research Institute of Petroleum Exploration and Development, Shengli Oilfield, SINOPEC, Dongying, China, [3]Department of Earth and Environmental Sciences, University of Texas at Arlington, Arlington, TX, United States

OPEN ACCESS

Edited by:
Shang Xu,
China University of Petroleum, China

Reviewed by:
Rui Yang,
China University of Geosciences Wuhan, China
Chao Liang,
China University of Petroleum, Huadong, China

***Correspondence:**
Shun Zhang
satisfactoryshun@163.com

Specialty section:
This article was submitted to Economic Geology, a section of the journal Frontiers in Earth Science

Received: *19 January 2022*
Accepted: *07 March 2022*
Published: *14 April 2022*

Citation:
Liu H, Zhang S, Liu Y, Zhang P, Wei X, Wang Y, Zhu D, Hu Q, Yang W, Tang D, Ning F, Guan L and Bao Y (2022) Characteristics of Lithofacies Combinations and Reservoir Property of Carbonate-Rich Shale in Dongying Depression, Eastern China. Front. Earth Sci. 10:857729. doi: 10.3389/feart.2022.857729

Drilling has demonstrated that oil can be produced from the lacustrine shale in the upper part of the fourth member of the Shahejie Formation (Es4s) in Dongying Depression. These wells are often drilled in multiple lithofacies combinations, rather than a single lithofacies. Thus, it is necessary to classify the shale lithofacies combinations to optimize favorable exploration targets. The basic characteristics of carbonate mineral-rich shales in the Es4s were determined by core description, optical microscopy of thin sections, mineral analysis by X-ray diffraction, and scanning electron microscope analysis of argon ion-polished samples, combined with organic geochemical analysis and reservoir property analysis. The depositional setting was determined, and the lithofacies combinations of the shale were divided based on the depositional setting and vertical changes in lithofacies combination. Lithofacies combinations include 1) laminated argillaceous limestone interbedded with the calcareous mudstone (LLM); 2) laminated argillaceous limestone interbedded with dolomite (LLD); and 3) calcareous mudstone intercalated with argillaceous limestone (BML). LLM formed in a semi-humid climate, with limited detrital provenance, while LLD was mainly the product of an arid climate, little detrital input, semi-deep water, and a strongly reducing saltwater environment. In addition to the basal strata in the center of the depression, the LLD lithofacies combination was also widely developed on the gentle slope and the slope area transitional to deep depression in the south of the basin. BML was mainly formed in a semi-humid climate, brackish, deep water, and a reducing environment with many detrital provenances. The porosity in LLM and LLD consists of various types. Intercrystalline pores in clay minerals, intercrystalline pores and dissolution pores in carbonate minerals, interbedded fractures, and ultra-pressure fractures are well developed. The pore width distribution range of both LLM and LLD is large. The porosity of LLM is slightly higher than that of LLD. Interlayers with higher dolomite content have higher permeability. The types of pores in BML with no significant laminae characteristics are less abundant, and it is difficult to form an effective reservoir porosity network from the pores and microfractures, and hence, the reservoir physical properties are relatively poor. Oil saturation index indicates that both LLD and LLM of medium–low degree of evolution have good oil content.

Keywords: Dongying Depression, Paleogene, shale oil, lithofacies combination, sedimentary environment

1 INTRODUCTION

At present, the research on shale oil and shale gas has entered a rapid development stage, and its main driving force comes from the commercial breakthrough of shale oil and gas in major oil-bearing basins all over the world. Until now, only the United States, Canada, and China have got the commercial development of shale oil and gas. From the current China shale oil and gas breakthrough, the southern marine shale represented by the Sichuan Basin mainly produces shale gas, while the continental shale widely distributed in the north mainly produces oil. The oil resource potential of continental organic-rich shale in northern China has been clearly verified. The continental organic-rich shale represented by the Shahejie Formation and Kongdian Formation in the Bohai Bay Basin, Yanchang Formation in the Ordos Basin, and Nenjiang Formation and Qingshankou Formation in the Songliao Basin are the main source rocks for conventional oil and gas accumulation in the basin.

Recognition of the different lithofacies is an important step in the evaluation of shale oil and gas, flow capacity, and mechanical properties (Hickey and Henk, 2007; Loucks and Ruppel, 2007; Maiti et al., 2007; Chen et al., 2016). Lithofacies is the macroscopic manifestation of shale material composition. Different lithofacies types represent the differences of shale organic matter abundance, mineral composition, reservoir space, and oil–gas potential. It can be seen from the summary of the research on the relative oil content, reservoir space, and production of shale that the sedimentary structure and components of shale have always had a direct impact on the reservoir space of shale (Chen et al., 2016; Han et al., 2016; Tang et al., 2016; Chen et al., 2019; Su et al., 2019; Li et al., 2021). When a single lithofacies reaches a certain thickness, which meets the requirements of fracturing engineering, geology, and engineering, we can use a single lithofacies as an evaluation or research unit. By comparing the rich organic shale in different sedimentary basins in China, the previous study found that the continental shale has higher heterogeneity than the marine shale (Yang et al., 2017). The macroscopic aspect shows that the lithology of continental shale changes in higher frequency vertically and horizontally, whereas the microscopic aspect shows that there are obvious differences in rock components and reservoir physical properties caused by rapid lithology changes. The strong heterogeneity brings difficulties to the division of shale oil research/evaluation units. Because the shale formation is considered to exist in large areas, the division of characterization units not only needs to solve the problems of evaluation and engineering development but also needs to have geological significance to guide the exploration work. Therefore, it is a challenge for shale oil evaluation to divide clear characterization units in continental shale series.

In 2020, Shengli oil field company found highly productive oil-bearing shale in the carbonate-rich shale in the fourth member of the Paleogene Shahejie Formation (ES4S) in the Dongying Depression. Production has exceeded ten thousand tons in the overpressured shale at early-peak oil-window maturity (vitrinite reflectance <0.9%). In the Mesozoic strata and Cenozoic strata of continental faulted basins, the organic-rich shale strata are highly heterogeneous (Zhang et al., 2009a; He et al., 2016; Ma et al., 2017). The Donying Depression in the Bohai Basin is such an example (Liang et al., 2017; Liu et al., 2017), where shale deposition was affected by the changeable lacustrine depositional setting. Well results have shown that the shale facies in the Dongying Depression changes significantly over a few kilometers horizontally, and there are cyclical changes over a few meters or even centimeters vertically (Wang et al., 2016). Therefore, research limited to the lithofacies scale, either vertically or laterally, is not applicable to the needs of shale oil production in such continental faulted basins. Different types of shale lithofacies need to be analyzed, combined, and classified at the sedimentary basin scale, so as to identify effective units for drilling and fracturing.

The Es4s shale series in the Dongying sag of the Bohai Bay Basin were taken as the research object. Combined with the observation with naked eyes, optical microscope and field emission scanning electron microscope (FE-SEM), the analysis of the X-ray diffraction (XRD), and the analysis of inductively coupled plasma-atomic emission spectrometer (ICP-AES), the depositional setting of the ES4S shale over time has been established. Shale strata were divided into lithofacies combinations based on the differences in depositional setting. Based on the rock pyrolysis data, the oil-bearing characteristics of the main lithofacies combination were analyzed.

2 GEOLOGICAL SETTING

The Bohai Bay Basin is developed on the top of the Paleozoic North China Craton basement in eastern China (**Figure 1A**), a region consists of several subbasins divided by uplifts. During the Cenozoic era, the Bohai Bay Basin underwent several distinct phases of rifting and subsidence (Allen et al., 1997), resulting in thick Paleogene, Neogene, and Quaternary lacustrine deposits. The Dongying Depression, which is located in the southeast of the Bohai Bay Basin, was developed as a result of the Cenozoic rifting (Feng et al., 2013). It has a total area of 5,700 km^2, and is bordered by the Chengning Uplift to the north, the Luxi Uplift to the southeast, the Gaoqing Uplift to the west, the Linfanjia Uplift to the northwest, the Qingtuozi Uplift to the northeast, and the Guangrao Uplift to the southeast (**Figure 1B**). Controlled by the structure unit four sags were developed in the Dongying Depression: Minfeng sag, Lijin sag, Niuzhuang sag, and Boxing sag. Paleogene synrift strata of the depression rest unconformably on pre-Paleogene strata. Neogene postrift strata rest unconformably on pre-Neogene strata; the succession of Paleogene synrift strata is typically 4,000–7,000 m thick (Zong et al., 1999). The tectonic evolution of the Dongying Depression comprised a rifting stage and post-rifting thermal subsidence. Thus, the initial rifting stage can also be subdivided into four rifting episodes (**Figure 1**): Rifting I (65–50.4 Ma), Rifting II (50.4–42.5 Ma), Rifting III (42.5–38 Ma), and Rifting IV (38–24.6 Ma). Within the Rifting II and Rifting III periods, the lake basin subsided rapidly and

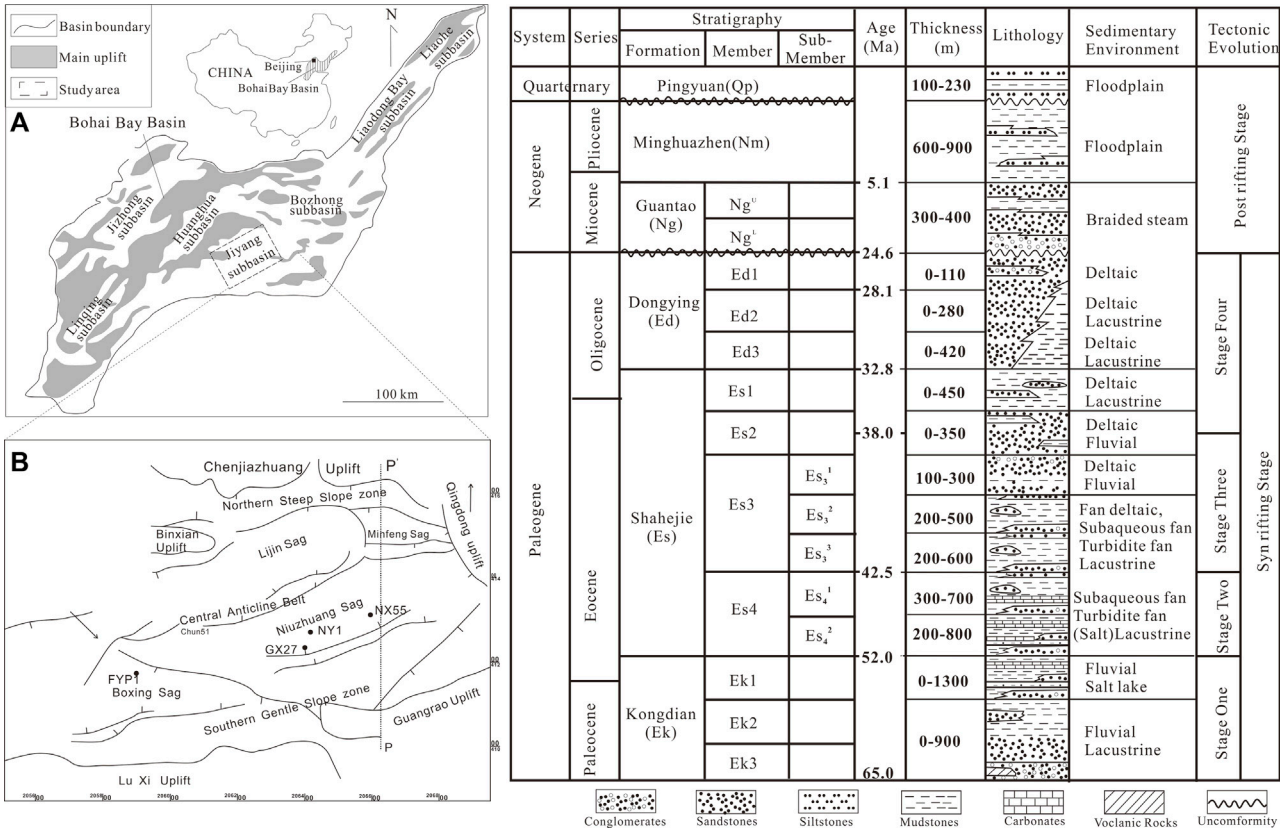

FIGURE 1 | Location map of study area. **(A)** Structural map of Bohai Bay Basin; **(B)** structural map of the Dongying Depression showing key well locations.

large-scale lake expansion occurred (Ma et al., 2016; Ma et al., 2017), leading to the organic-rich deposits in large area. During this period, two sets of thick and high-quality source rocks were developed in the Es4s and the Es3x (Zhang et al., 2009b) and the thickness of source rocks in the Es4s can reach 100–350 m.

3 MATERIALS AND METHODS

The basic data used in this study include more than 400 m of drill cores and 400 samples thin sections from four wells (FYP1, NY1, NX55, and NY1, **Figure 1B**). Forty field emission scanning electron microscope (FE-SEM) samples, 71 rock pyrolysis analyses, 71 maceral compositions analyses, 78 organic carbon analyses, and 78 X-ray diffraction (XRD) samples, 8 NMR analyses.

Core samples from four wells, including one horizontal well (FYP1) and two deviated wells (GX27 and NX55), from two sags were selected for the current study; they are considered to be geographically representative of the entire territory of the Dongying Depression. All of the analyses were carried out at the Exploration and Development Institute of Shengli Oilfield Company (SINOPEC).

For XRD analyses, powdered samples were oven-dried at 40°C for 2 days. Samples were then placed in copper holders and scanned using a D8 DISCOVER X-ray diffractometer. The generator settings of the diffractometer were 40 kV and 25 mA. Samples were scanned from 3° to 70° at 2°/min with a step width of 0.02° and using Cu-Kα radiation and a secondary graphite monochromator for rock composition.

TOC wt% of the samples were analyzed using a LECO CS-600 carbon/sulfur analyzer. Analytical precision for TOC analyses is better than ±0.5%. The concentrations of elements Al, K, and Na were also analyzed using an inductively coupled plasma-atomic emission spectrometer (ICP-AES) with an analytical precision of 0.5%. The powdered samples were digested using HF (40%) and mixture of HNO_3 (65%), $HClO_4$ (60%), and ultrapure H_2O before analyses.

Rock-Eval pyrolysis was performed on 200 mesh samples. During the pyrolysis the first peak (S1, mg HC/g rock) represents hydrocarbons distilled from rock. The second peak (S2, mg HC/g rock) represents hydrocarbons generated by pyrolytic degradation. Temperature of maximum pyrolysis yield (Tmax, °C) refers to the temperature at which the maximum amount of S2 hydrocarbons is generated.

A FEI Quanta 450 field emission scanning electron microscopy (FE-SEM) was used to observe the bulk samples with size of approximately 1*1.5 cm. An approximately 70-μm thickness of the surface material was removed using a Gatan Ilion II milling system with an accelerating voltage of 6–7 keV for 4.5 h,

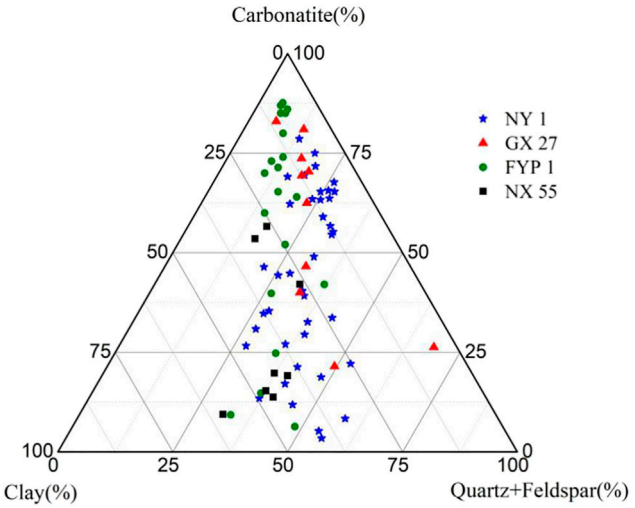

FIGURE 2 | Ternary plot showing the whole-rock mineral compositions of the Es4s shale in Dongying Depression.

and eventually, a flat surface with no gold or carbon cover was produced for the observation.

The NMR T2 distribution and T1–T2 map experiments were carried out on a MicroMR23-060H-1 instrument, with a frequency of 21.36 MHz, magnet strength of 0.28 T, and a testing temperature of 32°C. The Carr–Purcell–Meiboom–Gill (CPMG) sequence was used to obtain the T2 distribution, whereas the T1–T2 map was generated based on the Inversion Recovery (IR)-CPMG sequence.

4 RESULTS

4.1 Mineral Composition

The results of thin-section identification and x-diffraction analysis show that the shale of the fourth upper member of the Shahejie Formation in the Dongying Depression is mainly composed of carbonates, clays, quartz, feldspars, and other minerals, in additional to a small amount of pyrite (**Figure 2**; **Table 1**). The total content of carbonates, clay minerals, quartz, and feldspars in wells NY1, GX27, and NX55 accounts for 96.0, 98.1, and 85.7% of the whole-rock minerals, respectively (**Table 1**). Among them, the content of carbonate minerals mainly composing of calcite and dolomite is the highest, ranging from 5 to 97%, and the average content is close to or more than 50% (**Table 1**). The crystal forms of carbonate minerals are coarse crystals, micro-fine crystals and of cryptocrystalline. Calcite is mostly produced with organic-rich clay laminae or interbedded laminae mixed with clays and felsic minerals (**Figure 3**). Dolomite is mostly present as idiomorphic crystals, and the edge of dolomite is metasomatized by anhydrite (**Figures 3**, **5**). Quartz is mainly clay- to silt-sized minerals in two forms. The content of clay minerals is between 3 and 56%, with an average content of approximately 23%. The clay minerals are mainly illite/illite mixed layer and illite in flake or filamentous shape (**Figures 3A–C**), often mixed with terrigenous clasts of mud grade; in addition, the content of kaolinite and chlorite is relatively small (**Figure 3**). Pyrite is distributed in berry-like and pellet-like aggregates in mud or filled in biological shells, representing a strong reducing environment and moderate alkalinity with a pH value of 8–9.

4.2 Lithofacies Combination

Based on the analysis of the basic characteristics of the shale in the upper member of The fourth member of Shahejie Formation, the facies controlling theory of sedimentology, the characteristics of the paleoenvironments, the similarity of the sedimentary environment and the relative uniformity of the internal structure, and the superposition relationship of two or more kinds of vertical lithofacies, the lithofacies combinations of shale strata in the upper sub-member of the Shahejie Formation can be divided. The thickness of lithofacies combination is set as 30–50 m to meet the actual fracturing scale for horizontal well drilling and hydro-fracturing process for shale oil production. In general, the following types of carbonate mineral-rich shales are mainly developed in Dongying Depression: Laminated argillaceous limestone interbedded with the calcareous mudstone (LLM), laminated argillaceous limestone interbedded with dolomite (LLD), and bedded calcareous mudstone intercalated with laminated argillaceous limestone (BMLL).

4.2.1 Laminated Argillaceous Limestone Interbedded With the Calcareous Mudstone

LLM are the most developed lithofacies types of Paleogene in Jiyang Depression. Organic laminar (coarse-grained and fine-grained) argillaceous limestone is the most favorable reservoir lithofacies type, which is also considered the dominant lithofacies in the actual exploration practice. Laminar argillaceous limestone and calcareous mudstone are frequently interbedded, which constitutes the most developed lithofacies combination in the middle of the upper Es4 member. The microscopic image shows that the lamina features are remarkable (**Figures 4A–I**), most of which are straight, and the boundary between micrite/sparite lamina and organic-rich clay layer (or organic matter layer/clay layer) is clear, revealing a quiet water environment with few material sources and event sedimentary disturbances, good water stratification conditions, and relatively quiet water environment.

4.2.2 Laminated Argillaceous Limestone Interbedded With Dolomite

It is mainly developed at the bottom of the upper sub-member of Es4 in the center of the depression. The lithofacies include gray black laminated argillaceous limestone, light gray massive dolomite, and a small amount of laminated calcareous mudstone. Dolomite intercalation is mainly produced in blocks, with light gray color and thickness of 0.4–2.5 m. Thin-section observation and X-ray whole-rock mineral diffraction analysis are carried out for the intercalation part of massive dolomite. The mineral composition is mainly dolomite (micrite structure, accounting for 70–83%), and a small amount of argillaceous, pyrite. The particle composition is mainly sand debris. The recrystallization structure of some particles is unclear, which is

TABLE 1 | Mineral content, total organic carbon (TOC) content, and Rock-Eval parameters of the Es4s shale in Dongying Depression.

Well	Depth (m)	Mineral composition (wt%)						TOC	S1 (mg/g)	S2 (mg/g)	Tmax (°C)	Ro (%)
		Cl	%	F	Cal	Dol	Py					
GX27	2300.91	14	10	2	55	19	-	1.96	0.18	11.39	436	0.43
GX27	2301.90	17	10	0	70	3	-	6.30	1.84	46.08	435	-
GX27	2302.54	24	16	7	9	42	2	5.09	2.46	34.38	427	-
GX27	2303.18	25	13	2	57	3	-	3.67	0.35	15.28	435	-
GX27	2304.10	16	9	3	64	6	2	2.61	0.35	13.33	433	-
GX27	2305.02	39	24	10	24	-	3	5.96	0.63	45.04	436	-
GX27	2305.85	8	5	2	83	2	-	7.97	1.25	44.42	438	-
GX27	2306.86	19	11	4	50	14	2	11.30	2.56	79.71	429	-
GX27	2307.78	11	9	0	79	1	-	5.03	0.62	26.47	435	-
GX27	2308.02	43	29	17	5	1	5	10.10	0.44	78.14	443	-
GX27	2308.40	7	5	0	13	72	3	-	-	-	-	-
GX27	2309.22	8	5	0	75	12	-	5.82	0.15	7.40	440	-
GX27	2310.02	16	13	7	60	4	-	6.05	1.95	41.34	437	-
GX27	2310.82	9	6	0	82	3	-	4.58	0.20	8.84	437	0.48
GX27	2311.53	56	23	9	7	2	3	9.26	2.58	67.72	427	-
GX27	2313.14	7	6	1	82	4	-	4.50	0.40	14.68	435	0.43
GX27	2314.04	33	17	9	15	24	2	1.77	0.26	9.17	435	0.49
GX27	2315.29	21	29	8	23	19	-	0.77	0.06	3.41	440	-
GX27	2316.29	20	8	2	67	3	-	1.22	0.08	6.81	443	-
GX27	2317.29	46	25	10	3	11	5	5.07	1.18	33.30	427	0.50
FYP1	3451.65	26	25	6	18	20	5	3.67	1.67	14.80	452	0.78
FYP1	3454.15	11	5	1	78	5	-	-	-	-	-	-
FYP1	3456.19	5	28	40	23	3	-	0.62	1.89	2.26	441	-
FYP1	3457.55	6	11	2	68	13	-	0.85	1.84	2.63	445	-
FYP1	3462.95	12	16	2	56	12	2	1.02	1.42	3.16	449	-
FYP1	3465.08	10	12	4	61	12	1	1.01	2.81	4.41	439	-
FYP1	3468.81	20	19	8	33	8	11	4.69	2.21	15.12	450	-
FYP1	3470.55	14	18	4	43	17	4	1.31	0.99	3.85	453	-
FYP1	3471.40	10	17	2	62	7	2	1.43	1.08	4.55	451	-
FYP1	3473.57	27	32	14	9	11	6	5.37	1.75	20.87	454	0.83
NX55	3783.69	25	17	13	19	21	3	2.83	4.71	9.83	443	-
NX55	3784.60	30	10	6	45	8	-	-	-	-	-	-
NX55	3785.43	37	16	16	9	8	4	2.46	1.18	7.46	446	-
NX55	3785.79	26	13	4	49	7	1	0.90	1.04	1.70	439	-
NX55	3787.09	36	20	16	8	9	4	0.58	0.24	0.69	429	-
NX55	3787.85	37	16	16	6	5	-	0.52	0.17	0.74	449	-
NX55	3788.89	57	21	9	6	3	1	0.53	0.23	0.75	437	-
NX55	3790.40	40	12	20	6	7	4	0.87	0.75	1.88	446	-

Cl, clay; Q, quartz; F, feldspar; Cal, calcite; Dol, dolomite; Py, pyrite; TOC, remnant organic carbon; S1, free hydrocarbon; S2, pyrolyzed hydrocarbon.

suspected to be algae (**Figure 4I**, J, K, and L). It is speculated that the formation of dolomite interlayer is related to biogenesis. On the whole, the lithofacies combination is mainly developed in dry, less material source and salt water environment.

4.2.3 Bedded Calcareous Mudstone Intercalated With Laminated Argillaceous Limestone

This kind of lithofacies combination is mainly developed in the middle and upper part of the upper Es4 sub-member of Boxing sag and Niuzhuang sag. The core is characterized by mutual layers of organic-rich layered argillaceous limestone facies and organic-rich layered calcareous mudstone. In addition, a small amount of laminated argillaceous limestone is occasionally developed. Under the microscope, the main minerals show directional or weak directional fabric, and the size of plaster lens is different (200–500 μ m). Gypsum is distributed sporadically in lenticular shape (200-500). It can be seen that a small amount of felsic minerals are sporadically distributed, and laminae with good continuity is locally developed in the lithofacies (**Figure 4D**), which is characterized by mixed deposition of a variety of minerals as a whole. Compared with other lithofacies combinations, the lamina is underdeveloped, which reveals that the water depth, salinity, and stratification are weaker than that of laminar shale facies assemblages.

4.3 Organic Matter Content, Type, and Maturity

The results of geochemical analyses show that the abundance of organic matter is high and the distribution range is wide. The main organic carbon content of shale in the upper sub-member of the fourth member of the Shahejie Formation in the Dongying Depression ranges from 1.5 to 9.38%, and the highest is 11.4%

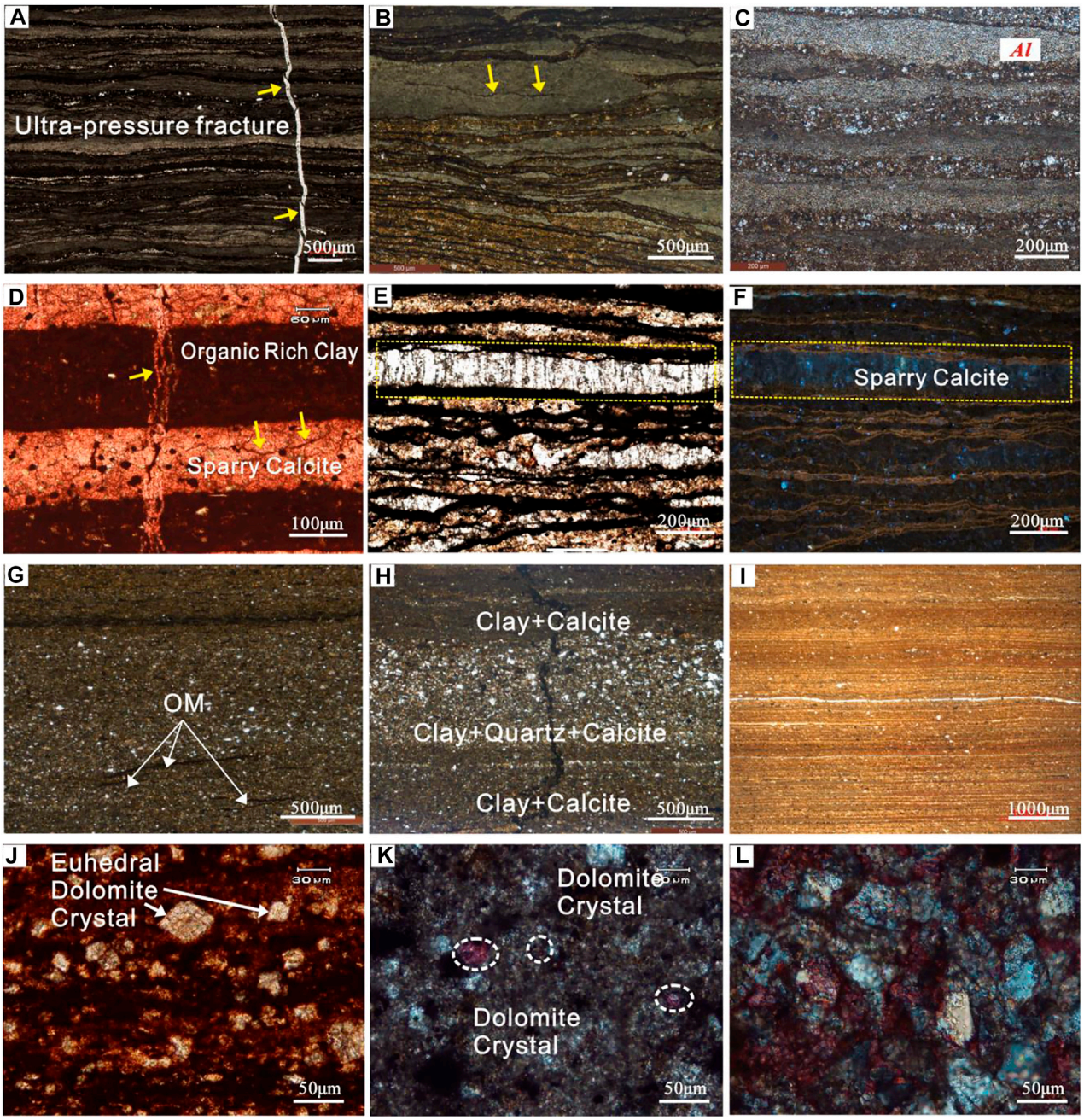

FIGURE 3 | Thin-section photomicrographs of the Es4s shale in Dongying Depression. **(A)** Organic-rich laminated argillaceous limestone, well FYP1, 3471.40 vm; **(B)** organic-rich laminated argillaceous limestone, well FYP1, 3458.00 m; **(C)** organic-contained laminated argillaceous limestone, well FYP1, 3457.55 m; **(D)** organic-rich laminated sparry limestone, ultra-pressure fracture, and calcite incrystalline pores, well NX55, 3785.79 m; **(E)** organic-rich laminated sparry limestone, well NX55, 3784.60 m, **(F)** fluorescent thin section; **(G)** and (H) layered calcareous mudstone, well NX55, 3785.43 m; **(I)** organic-rich laminated argillaceous dolomite, well GX27, 2302.54 m; **(J)** euhedral dolomite crystal, well NX55, 3785.43 m; **(K), (L)** calcite and dolomite crystals, well NX55, 3785.43 m.

(**Table 1**). The occurrence of organic matter in shale includes bedding enrichment type, bedding dispersal type, and mineral asphalt matrix. For organic-rich shales, organic matter is often laminated or curved in lines between carbonates and clays (**Figures 3E–G**), and it is easy to be recognized under optical and fluorescence microscopes. The organic matter types are mainly sapropelic, rich in algae fossils, which is a good quality source rock. The overall evolution degree of the upper Es4 shale in the Dongying Depression is medium to low, and the Ro value is between 0.5 and 1.3% to be mainly in oil generation window.

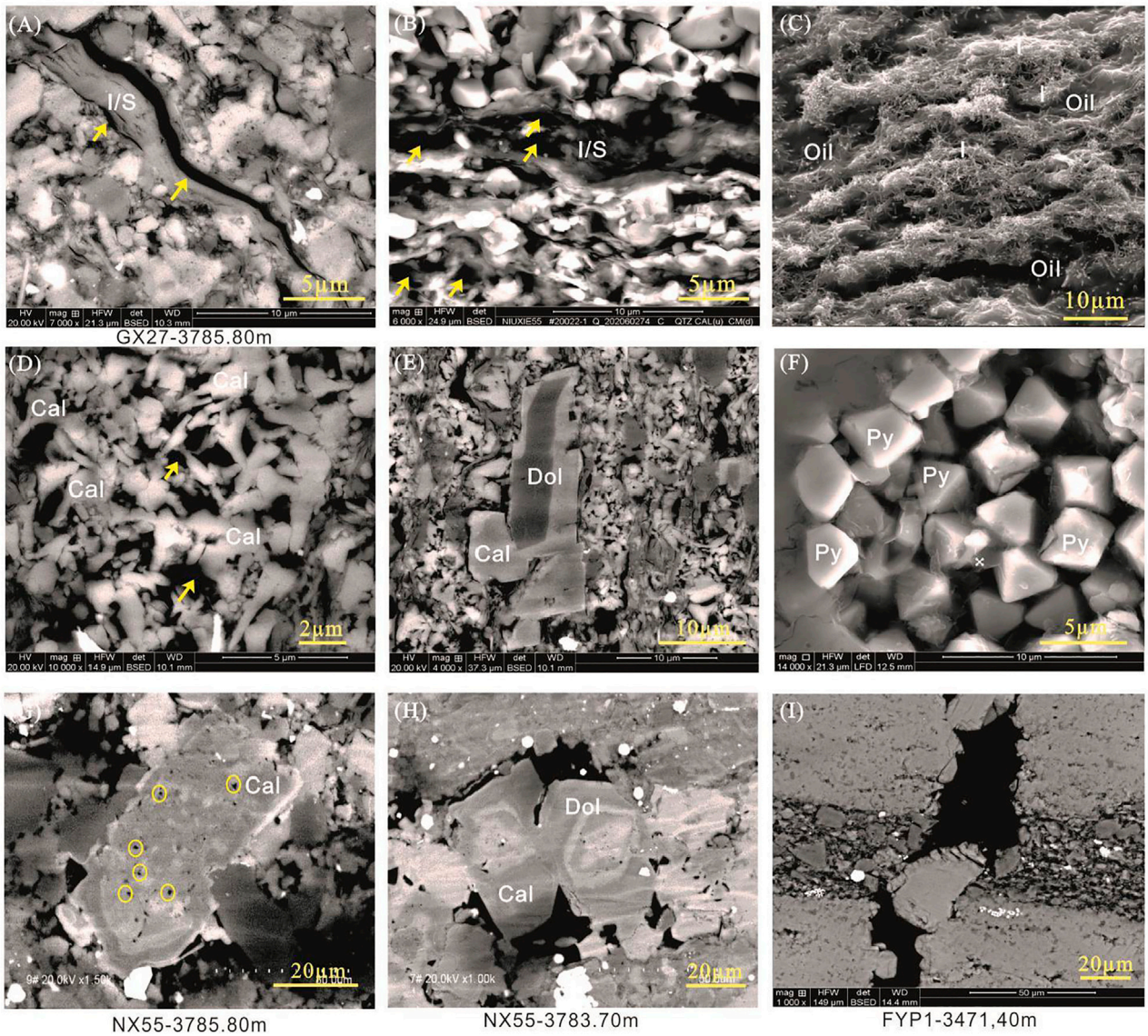

FIGURE 4 | FE-SEM images of Es4S shale in Dongying Depression. **(A)** I/S mixed layer shrinkage fracture, well GX27, 3785.80 m; **(B)** intercrystalline pores of clay minerals, well NX55, 3784.60 m; **(C)** filiform Illite incrystalline pores, well NY1, 3402.73 m; **(D)** calcite incrystalline pores, well FYP1, 3457.55 m; **(E)** incrystalline pores of calcite and dolomite, well FYP1, 3457.55 m; **(E)** incrystalline pores of pyrite, well GX27; **(F)** calcite intragranular dissolution pores, the mineral edge is partially dissolved and filled with organic matter, well NX55, 3785.80 m; **(H)** intergranular dissolution pores, well NX55, 3783.70 m; **(I)** seam-shaped dissolution, dissolution pores between calcite particles, well FYP1, 3471.40 m. I/S is illite and semctite mix layer, Cal is calcite, Dol is dolomite, Py is pyrite.

4.4 Reservoir Characteristics Observed With SEM

In general, pores associated with inorganic minerals are dominant (**Figure 4**), and pore combinations are formed by organic pores and intercrystalline pores of clay minerals. Fracture types are mainly developed interlayer microfractures and ultra-pressure fractures (**Figure 3**), and pore types mainly included clay mineral intercrystalline pores (**Figures 4A–C**), calcite intercrystalline pores (**Figures 4D, E**), and dissolution pores (**Figures 4G–I**), and the pore widths are concentrated in 3 nm–10 μm. Intercrystalline pores of clay minerals are mainly developed in illite and smectite mixed beds (**Figures 4A–C**), and the crystal shapes are mostly lamellar, lamellar, and fibrous. Micropores generated during illitization are an important part of intercrystalline pores of clay minerals. The most common solution pores are calcite solution pores, which are mainly developed in and between granular calcite grains (**Figures 4G, H**). A small amount of dolomite solution pores can also be seen in

the dolomite-concentrated development zones. Interlaminar pores and fractures are more likely to occur in fine-grained sedimentary rocks with densely developed carbonate laminae. In argillaceous limestone containing coarse-grained calcite, the higher the calcite content, the more developed the recrystallized intercrystalline pores and fractures are, and the more favorable they are for oil and gas accumulation. In addition, closed pores of pyrite are common (**Figure 4F**).

5 DISCUSSION

5.1 Palaeoenvironmental Characteristics

5.1.1 Paleoenvironment Restoration

The lacustrine shale has the characteristics of complex components, diverse types, and uneven distribution, which reflects the variability of the formation environment of the terrestrial shale fine-grained deposition. The analysis of sedimentary environment includes five aspects: paleoclimate, paleoprovenance, paleowater depth, paleosalinity, and oxidation reduction of paleowater. At present, the methods of geochemical elements and mineral content are widely used to restore the sedimentary environment.

Climate is often expressed by temperature and humidity. Among the geochemical elements, Ca, Mg, Na, K, Sr, and Ba indicate the dry climate, while Fe, Mn, Cr, V, Co, and Ni indicate the wet climate. As the ratio of Sr/Mg, Mg/Ca, and Sr/Ca decreased, the corresponding temperature increased; in contrast, when the ratio is increased, the corresponding paleo-temperature decreases. A high Ba/Sr ratio indicates a warm and wet climate, rather than a dry and cold climate (Peng et al., 2012). The migration and enrichment of elements is not only related to the physical and chemical properties of the elements themselves, but also closely related to the geological environment. Therefore, the use of multiple elements reflects the sedimentary environment at that time more accurately. According to the corresponding relationship between the elements and the drought or wet climate, the concept of paleoclimate index is introduced. The paleoclimate can be quantitatively analyzed (Guan, 1992). C = $\sum$ (Fe, Mn, and Cr + V + Co + Ni)/$\sum$ (Ca, Mg, and Sr + Ba + Na +, K +) type in C for the ancient climate index. The greater the value of C indicates a warm and wet climate, whereas the opposite indicates a dry and cold climate.

Salinity refers to the mass fraction of all soluble salts in the medium. Paleosalinity recovery is one of the important methods for paleoenvironment and paleoclimate study. At present, the Couch formula is relatively complete and widely used to calculate paleosalinity (Couch, 1971), which can adapt to a wide range of salinity. It is mainly calculated based on the content of boron and clay minerals, and considers the influence of illite, montmorillonite, and kaolinite on the adsorption of boron (Walker, 1968). According to the salinity classification standard established by Huang (1995) and the actual situation of the study area, the salinity classification standard is established as follows: 0.5–1.0‰ is fresh water, 1.0–5.0‰ is brassy water, 5.0–15.0‰ is brassy water, and 15.0–30.0‰ is salty water. 30.0–50.0‰ was saline.

Geochemical elements can reflect the size of relative paleowater depth, and more Fe/Co is used in practical applications. The content of element Co increases with the deepening of water body. In general, as the water depth increases, the free oxygen in the lake decreases and the reducing condition gradually increases. The ratio of Fe/Co can indicate the relative depth of the ancient lake, and the value of Fe/Co is inversely proportional to the relative water depth.

Ancient source mainly refers to terrestrial source supply. In general, carbonate rocks are primary and clay minerals and felsic minerals are terrigenous inputs. Therefore, the percentage of clay + felsic minerals can be used to represent the amount of ancient source supply. According to the mineral composition and provenance characteristics of ES4s shale in Dongying Depression, the provenance supply standard is divided as: ≥65% is more provenance, 50–65% is more provenance, 35–50% is less provenance. Provenance of the Dongying Depression is mainly concentrated in 20–70%. From the bottom to the top of Es4s, the provenance gradually increases.

5.1.2 Paleoenvironmental Characteristics of Carbonate-Rich Shale

Well NY 1 is a systematic core well in Dongying Depression. According to the result of a large number of element test and mineral analysis sampled systematically, the paleoenvironment of upper Es4 shale can be restored (Yang et al., 2015). According to the paleowater depth recovered by Fe/Co and the Th/U ratio method and previous research results, the water depth of the upper member of the fourth member of the Shahejie Formation in the Dongying Depression is 0–30 meters, and the magma rock is developed at the bottom of the shale section (Yang et al., 2018; Su et al., 2019). The upper member of the fourth member of the Shahejie Formation in the Dongying Depression can be divided into shallow lake facies, semi-deep lake facies, and deep lake facies from bottom to top. The subhumid and humid 2 climatic cycles were developed from the top to the bottom, and the climate changed from drought to humidity (**Figure 5**). There are three provenance supply cycles with less provenance and more provenance from bottom to top in the upper sub-member of the fourth member of the Shahejie Formation in Dongying Depression, and provenance has an increasing trend on the whole. In terms of water environment, the saline, saline, and brackish water environment are in order from bottom to top.

The Dongying Depression is an enclosed lake basin in Es4s, which determines the characteristics of coevolution among sedimentary environment elements. Climate is the main reason for the change in the sedimentary environment. In the dry period of climate, the concentration of water makes the deposition dominated by chemical action, rich in carbonate, and gypsum rocks. During the period of subhumid to semiarid climate, the balance between the mechanical and chemical processes was reached, and the mimetic rock deposits were most developed, including the layered and laminar deposits of organic-rich argillaceous limestone and calcareous mudstone (**Figure 6**). In humid period, due to abundant water injection and abundant provenance supply, terrigenous detritus deposited mainly by mechanical deposition and layered or massive

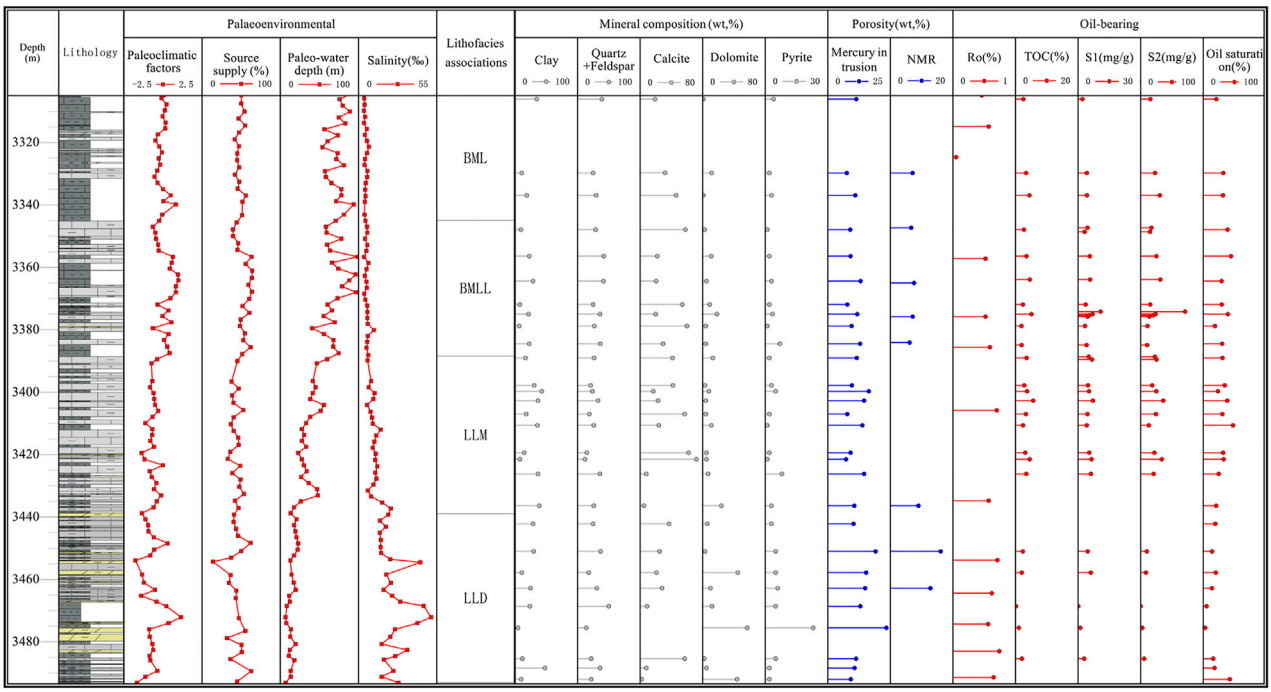

FIGURE 5 | Paleoenvironment analysis and characteristics of shale lithofacies combinations in well NY1: 1) bedded calcareous mudstone intercalated with laminated argillaceous limestone (BML), 2) bedded calcareous mudstone intercalated with laminated argillaceous limestone (BMLL), 3) laminated argillaceous limestone interbedded with the calcareous mudstone (LLM), 4) laminated argillaceous limestone interbedded with dolomite (LLD).

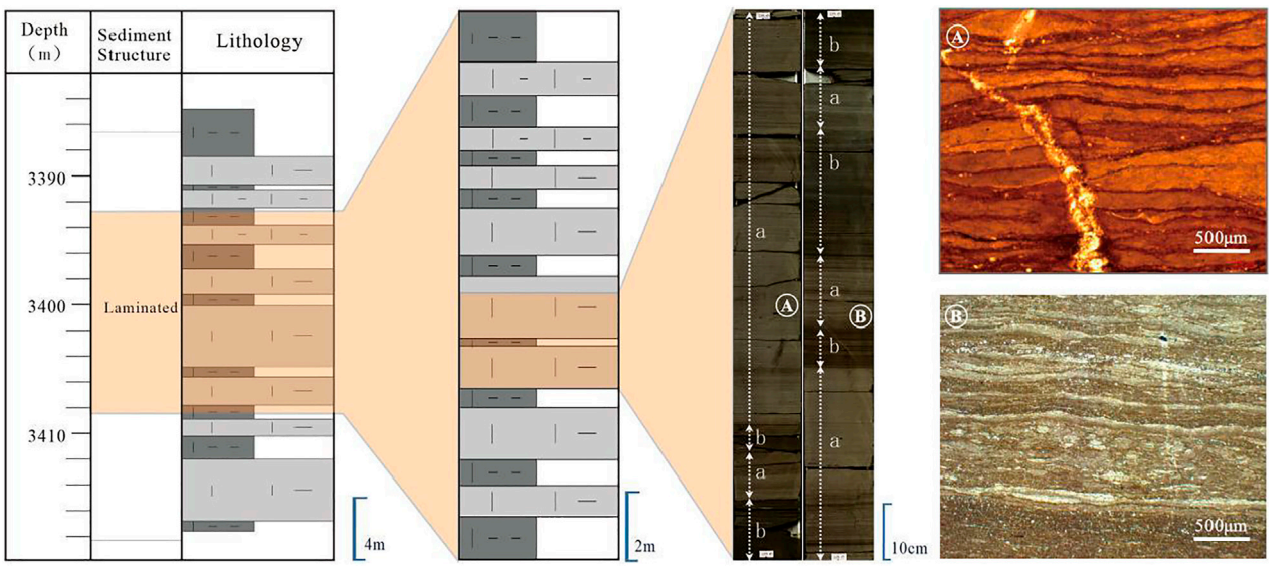

FIGURE 6 | Core observations and thin-section characteristics of lithofacies combination LLM.

calcareous mudstone containing (or rich in) organic matter were mainly developed. With the change in climate from dry to semidry to semi-wet conditions, the water body changed from semi-deep water to deep water, and the salinity changed from salt water to salt water to brackish water, the reduction of sedimentary environment gradually weakened, and the provenance increased (**Figure 5**). On the whole, the paleoclimate changed from subhumid to humid from bottom to upper, the detritus

provenance changed from few to many, the water body changed from shallow water to deep water, from salt water to briny water, and from strong reduction to reduction (**Figure 5**). In terms of lithofacies, the content of organic matter changes from less to more, the structure changes from laminar to layered, and the lithology can be successively dolomite-limestone-argillstone-calcareous mudstone-mudstone (**Figure 4**).

5.2 Characteristics of Shale Lithofacies Combinations

5.2.1 Laminated Argillaceous Limestone Interbedded With the Calcareous Mudstone

1) Characteristics of the sedimentary environment

Combined with the analysis of sedimentary environment indexes, it is indicated that the organic-rich laminated argillaceous limestone facies and organic-rich laminated argillaceous mudstone facies were formed in similar environments, and they often coexist in the study area and were mainly formed in the reducing environment with semidry climate and semi-deep water. The multi-episodic turbulent saltwater environment provides a large amount of soluble inorganic carbon, which lays a foundation for the massive crystallization precipitation and preservation of carbonate. According to the crystal structure and morphology, the carbonate laminae of laminated argillaceous limestone can be divided into micritic calcite laminae and sparry calcite laminae.

With respect to the differences of paleoenvironmental indicators, organic-rich laminated microrite-sparry limestone and argillaceous limestone combinations were formed in semi-humid, less provenance, semi-deep lake, and strong reductive saltwater environment, the organic-rich laminated micritic limestone and argillaceous limestone are formed in brackish water environment. On the whole, the sedimentary sequence developed in this environment is composed of organic-rich laminated micritic argillaceous limestone facies, organic-rich laminated micritic argillaceous limestone interbedded with organic-rich laminated calcareous mudstone from bottom to top. With the decrease of water salinity, carbonate crystals are dissolved and produced in micrite lamellar form.

2) Reservoir characteristics

The types of reservoir spaces are rich and varied, and the microfractures mainly include ultra-pressure fractures and bedding fractures. The pore types are mainly calcite grain intercrystalline pores and clay mineral intercrystalline pores, followed by dissolved pores. Most of the dissolved pores are developed in the interior of the particles, like round or oval, and are relatively isolated. The pore diameter is concentrated in the range of 1–2.5 μm, and the maximum is 5 μm. The intercrystalline pores of calcite recrystallization are generally between 20 and 40 μm, with the maximum of 100 μm and good connectivity. These near-horizontal pores form good channels for the flow and accumulation of hydrocarbon fluids. The calcite recrystallization intercrystalline pores (fractures) are formed by calcite crystal interstitial intercrystalline interstitial pores (fractures), which can form a very effective reservoir space network when they communicate with hydrocarbon-generating high-pressure fractures and shrinkage microfractures in the clay interbedded parts. Most dolomite in laminated is obviously the result of replacement of precursor calcite but certainly not all (**Figures 3G–I**), intergranular (dissolution) pores are commonly found in laminated argillaceous limestones containing dolomite crystals.

Data from nine sample sites showed porosity between 7.3–16.4%, with an average of 11.51%. Taking well NY 1 as an example, the NMR test shows that the porosity of the lithofacies combination is between 5.84 and 8.79%, and the porosity of laminated calcareous mudstone is slightly higher than that of laminated calcareous mudstone. The pore number of large pore width is positively correlated with the mass content of carbonate minerals.

The recrystallized portion of calcite is associated with organic-rich lime-black clay rocks developed in foliation, which has been proved in many studies. Calcite recrystallization is closely related to hydrocarbon generation of kerogen and shrinkage of clay minerals.

3) Oil-bearing and shale oil mobility

The average TOC is 3.36%, the average S1 is 4.72 mg/g, the average S2 is 15.99 mg/g, and the average hydrocarbon potential (S1 + S2) is 20.71 mg/g. The kerogen macerals are mainly sapropelites. The range of burial depth is concentrated, so the R_o value of thermal evolution is distributed in a small range, between 0.5 and 1.5%. The high abundance of organic matter and appropriate maturity conditions provide sufficient shale oil resources for shale matrix, and the lithofacies combination is basically in the main oil generation window. Oil saturation index (OSI) (S1/TOC × 100) can usually be used as an indicator to judge whether shale has movable resource potential. When OSI is at a certain value, shale oil reaches adsorption equilibrium and free oil exists. Pepper and Corvi, (1995) and Jarvie et al. (2012) used the relationship between pyrolysis parameter S1 content and TOC to study the lower limit of hydrocarbon adsorption of shale, and believed that the shale section with S1/TOC over 100 mg/g was favorable (Pepper and Corvi, 1995; Zhu et al., 2019). From the perspective of hydrocarbon reservoir generation and expulsion, carbonate minerals can promote the condensation and dehydrogenation of kerogen and improve the yield of hydrocarbons.

5.2.2 Laminated Argillaceous Limestone Interbedded With Dolomite

1) Characteristics of the sedimentary environment

The rock types developed in this lithofacies combination are complex, including argillaceous limestone, argillaceous mudstone, calcareous dolomite, and dolomitic limestone in terms of mineral composition (**Figure 5**). The dolomite is mainly produced in the form of interlayers, with a thickness of 30–150 cm. The typical sedimentary structure features are

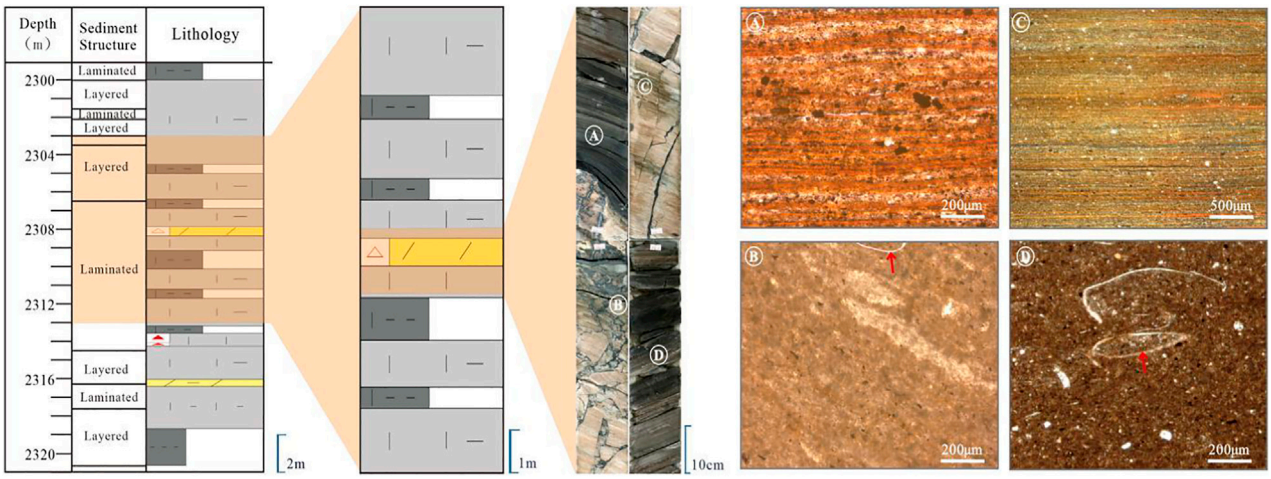

FIGURE 7 | Core observations and thin-section characteristics of lithofacies combination LLD.

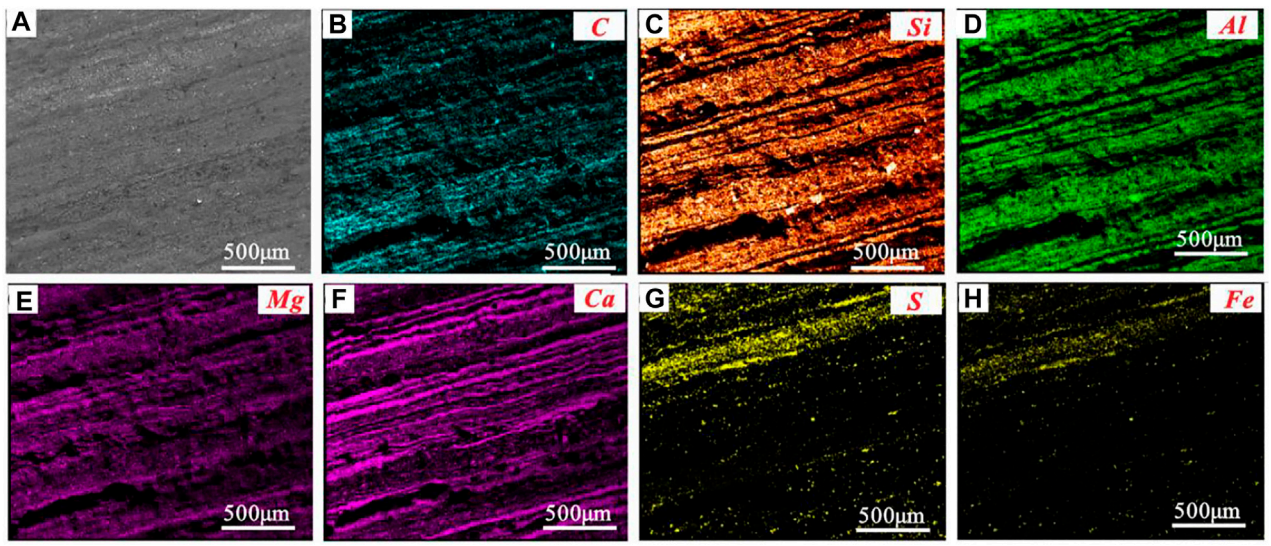

FIGURE 8 | Electron probe element scanning image of laminar argillaceous limestone (GX27, 2317.29 m): **(A)** secondary electron image; **(B–H)** element distribution diagram of carbon, silicon, aluminum, magnesium, calcium, sulfur, and iron, respectively.

laminar or layered. The lithofacies are of various types, mainly the organic-rich laminar argillaceous limestone facies and laminar argillaceous dolomite facies. The characteristics of environmental parameters show that the lithofacies combination is mainly the product of dry climate, little provenance, semi-deep water, and strong reducing environment of salt water and brackish water. The average Sr/Ba ratio was 5.27. According to the comprehensive column chart of typical wells (**Figure 5**), the lithofacies combination is mainly developed vertically in the middle and lower part of shale strata of the upper sub-member of the fourth member of the Shahejie Formation in the central depression of the southern basin (**Figure 1**), and mainly developed horizontally in the gentle slope zone of the southern fault basin (**Figure 1**). In general, it is mainly characterized by laminar argillaceous limestone interbedded with argillaceous dolomite.

Taking well GX27 in the southern gentle slope zone of the Dongying Depression as an example (**Figure 7**), the upper sub-member of the fourth member of the Shahejie Formation mainly develops gray black laminar argillaceous limestone with brown laminar dolomite (**Figure 7**). Under the microscope, small oamoeba with thin shells can be seen, and some of them are produced in a long axis direction (**Figures 7B,D**, **8**), reflecting the semi-deep water environment with certain hydrodynamics. The

paleoenvironmental parameters show that the dry-wet index of the dolomite-concentrated development section reaches the lowest (<0.1), and the provenance supply capacity is slightly higher than that of the lithologic facies combination of well NY 1 near the center of the secondary subsag (<35%) because it is close to the provenance supply area of the southern gentle slope (**Figure 7B**).

2) Reservoir characteristics

Owing to the relatively common dolomite, dolomite intercrystalline pores can be observed by scanning electron microscope, and dissolution pores can be seen at the edge or corner of calcite and dolomite, which are mostly polygonal or irregular shape. Some fractures are filled with organic matter and dolomite, and the dolomite is relatively idiomorphic (**Figure 3G**). Part of the dissolution pores are filled with dolomite and organic matter, and the self-shaped edge of the dolomite is irregular metasomatized (**Figure 3K**). According to the core observations, the macro fractures in the dolomite interlayer are relatively developed (**Figure 7**), and the fractures are mainly extended along the bed, with a small number of oblique fractures and near-vertical ultra-pressure fractures, and the width of the fractures is concentrated in 0.01–0.5 mm. In addition, some samples showed pelletic pyrite intercrystalline pores and organic matter shrinkage fractures (**Figure 4F**).

In terms of reservoir physical properties, taking the 3440–3464 m depth section of well NY 1 as an example, the average porosity is 15% and the average permeability is 21 mD. The development of dolomite interlayer is the most typical characteristic of this lithofacies combination. In the previous study of shale in Dongying Depression, the dolomite interlayer has not been systematically analyzed. The reservoir physical properties of the dolomite-concentrated development section in well GX 27 were studied. Three kinds of lithofacies of Dolomitic mudstone, Dolomitic bearing calcareous mudstone, and argillaceous dolomite were found in well GX 27 and two samples are selected for each lithofacies for the reservoir physical properties study. The porosity was measured by the overburden pore infiltration method, the constant rate mercury injection method, and the pulse method. The results of porosity and permeability test of layered calcareous mudstone, dolomitic mudstone, and laminated argillaceous mudstone show that the dolomitic mudstone has the highest porosity and the argillaceous dolomite has the lowest porosity. However, permeability shows the opposite characteristics. CT scan results of laminar dolomite samples show that the average pore width of argillaceous dolomite is 330 nm, the average pore width of calcareous mudstone is 220.6 nm, and the average pore width of dolomitic mudstone is 203 nm. The results of nitrogen adsorption at low temperature show that the main pores of the samples are contributed by the pores between 40 and 80 nm. This also reflects that the interlayer with higher dolomite content has higher permeability and higher ratio of large pore width. It also shows that the unique supporting effect of dolomite in matrix pores is beneficial to the development of matrix pore and fracture system.

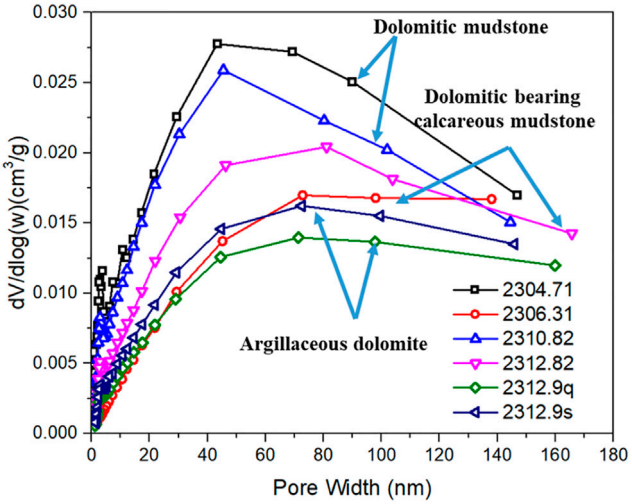

FIGURE 9 | Pore width distributions calculated from N_2 adsorption isotherm tests.

Data from N_2 adsorption show that all samples have similar distribution of pore width, with a peak at approximately 2.8 nm diameter (**Figure 9**). In addition, the specific surface area calculated by the multi-point BET method was 2.49–11.32 m^2/g, and the adsorption curve calculated by the BJH formula showed that the pore volume of the sample was 0.016–0.037 cm^3/g. The average aperture is 10.19–19.79 nm. Most of the pore diameters are less than 4 nm (**Figure 9**). Among the six samples, the core sample at 2304.71 depth has the most pore diameter less than 4 nm, followed by sample 2310.82 m, and the remaining samples have very limited pore diameter less than 4 nm.

3) Oil-bearing and shale oil mobility

TOC of this lithofacies combination in the southern gentle slope zone ranges from 1.77 to 6.05% with an average of 5.07%. The mean values of pyrolysis S1 and S2 are 4.72 mg/g and 15.99 mg/g, respectively. The average hydrocarbon generation potential (S1 + S2) was 20.71 mg/g; The pyrolysis S1 of this lithofacies combination in well GX27 in the southern gentle slope zone is generally low, with an average value of 0.92%, and an average value of S2 of 30.89%. The kerogen macerals are mainly sapropelites. Owing to the wide range of burial depth, the R_o range of thermal evolution degree is wide, ranging from 0.5 to 1.5%. The shallow burial depth and R_o range of 0.43–0.5% in the southern gentle slope of the basin, and the lithofacies combination is basically in the main oil generation window.

The measured oil saturation values of the lithofacies combination in well NY1 have a wide range, ranging from 5.3 to 55.5%, with an average value of 26.55%, OSI average. Rock slices and elemental analysis results also confirm that the lithofacies combination has good oil content. The figure shows laminar argillaceous microcrystalline limestone and brecciate calcareous dolomite with calcite intergranular pores filling asphaltene.

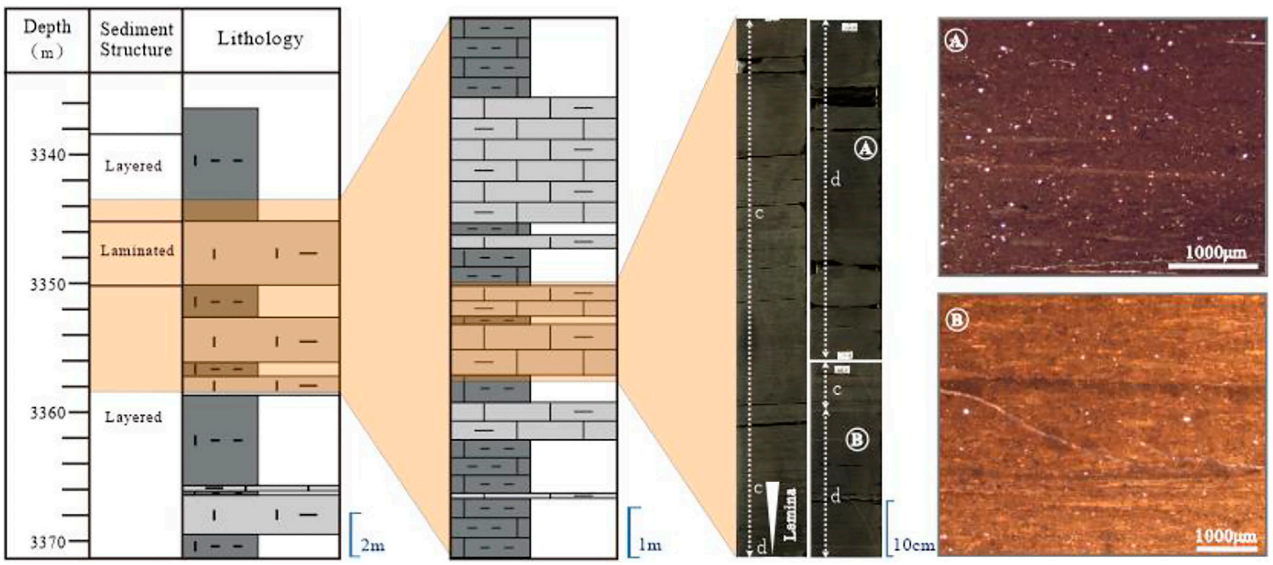

FIGURE 10 | Core observations and thin-section characteristics of lithofacies combination BML.

5.2.3 Bedded Calcareous Mudstone Intercalated With Laminated Argillaceous Limestone

1) Characteristics of the sedimentary environment

The bedded argillaceous limestone facies and bedded calcareous mudstone facies are mainly formed in semi-humid and brackish water deep water. The average Sr/Ba ratio is 2.24 and the average dry-wet index is 0.22 in the reduction environment with more provenance. Because the climate tends to be relatively wet, the water body is relatively deep, and the seasonal climate control deposition is weak, the shale is dominated by layered structures, with a small number of laminated structures developed, and compared with the lithofacies combinations A and B. But the boundaries of laminae are unclear and difficult to distinguish (**Figure 10**). A large amount of terrigenous clastic provenance input is also a typical feature of this lithofacies combination. The XRD whole-rock mineral diffraction data of more than 50 samples from 3350 to 3390 m in well NY1 show that the average mass content of quartz mineral is more than 30%, which is higher than that of the lithofacies combinations A and B.

On the whole, the sedimentary sequence of lithofacies combination developed in this environment is as follows from bottom to top: organic-rich layered argillaceous limestone, organic-rich layered calcareous mudstone interbedded with organic-rich layered calcareous mudstone, and organic-rich layered calcareous mudstone interbedded with organic-rich layered argillaceous limestone.

2) Reservoir characteristics

Due to the underdevelopment of laminae, the microscopic heterogeneity is weaker than that of shale with significant laminae characteristics. The stratified calcareous mudstone and calcareous mudstone samples observed under microscope show that the contact relationship between different types of minerals is close, and the average density of the directionally semi-directional fabric rock is 2.39. The pore types are mainly clay mineral intercrystalline pores and calcite intercrystalline pores. Small quartz crystals are distributed in calcite dissolution pores (2.5–3.5 μm in diameter), and a small amount of quartz and feldspar intergranular pores are also developed. Calcite recrystallized intercrystalline pores and dolomite dissolution pores are not common. The argillaceous layer is fracture width. In terms of reservoir physical properties, the conventional core analysis results show that the porosity is concentrated in 7.6–11%, with an average of 9.15%, and the average of the nuclear magnetic resonance test porosity is 6.865%. The horizontal permeability ranged from 0.3 to 8.28 mD with an average of 0.52 mD, which was related to the underdevelopment of laminated and bedding in lithofacies combination. The average vertical permeability was 0.092 m.

3) Oil-bearing and shale oil mobility

TOC values ranged from 1.4 to 4.4%, with an average value of 2.60%. The average value of S1 and S2 was 3.9 mg/g, 17.4 mg/g, and the average hydrocarbon generation potential (S1 + S2) was 21.4 mg/g. The kerogen macerals are mainly sapropelites. Due to the concentration of burial depth, the Ro range of thermal evolution is small, ranging from 0.5 to 1.5%, and the lithofacies combination is basically in the main oil generation window; the measured oil saturation values of this lithofacies combination in well NY1 are concentrated, ranging from 21 to 42.2%, with an average value of 35.45%. The oil saturation of layered calcareous mudstone is slightly higher than that of layered argillaceous limestone.

6 CONCLUSION

Based on the characteristics of the paleoenvironment, the lithofacies combinations of shale strata in the upper submember of The fourth member of the Shahejie Formation were divided according to the principles of the similarity of the sedimentary environment and internal structure and combined with the superposition relationship of two or more kinds of vertical lithofacies. Lithofacies combination includes laminated argillaceous limestone interbedded with the calcareous mudstone (LLM), laminated argillaceous limestone interbedded with dolomite (LLD), and bedded calcareous mudstone intercalated with laminated argillaceous limestone (BMLL). LLM formed in semi-humid, less provenance; LLD is mainly the product of dry climate, little provenance, semi-deep water, and strong reductive saltwater environment.

LLM and LLD reservoir spaces are of various types. The types of BMLL reservoir spaces with no significant laminae characteristics are less abundant, and it is difficult to form an effective reservoir space network with pores and microfractures, and the reservoir physical properties are relatively poor. Oil saturation and OSI indicate that both LLD and LLM of medium–low degree of evolution have good oil content.

DATA AVAILABILITY STATEMENT

The raw data supporting the conclusion of this article will be made available by the authors, without undue reservation.

AUTHOR CONTRIBUTIONS

HL and SZ as the first authors provided the idea and wrote the paper. YL, PZ and QH were responsible for handling technical problems. XW, YW, DZ, WY, DT, FN, LG and YB were responsible for experiment and data analysis.

REFERENCES

Allen, M. B., Macdonald, D. I. M., Xun, Z., Vincent, S. J., and Brouet-Menzies, C. (1997). Early Cenozoic Two-phase Extension and Late Cenozoic thermal Subsidence and Inversion of the Bohai Basin, Northern China. *Mar. Pet. Geology.* 14, 951–972. doi:10.1016/s0264-8172(97)00027-5

Chen, K., Liu, X., Liu, J., Zhang, C., Guan, M., and Zhou, S. (2019). Lithofacies and Pore Characterization of continental Shale in the Second Member of the Kongdian Formation in the Cangdong Sag, Bohai Bay Basin, China. *J. Pet. Sci. Eng.* 177, 154–166. doi:10.1016/j.petrol.2019.02.022

Chen, L., Jiang, Z., Liu, K., Wang, P., Ji, W., Gao, F., et al. (2016). Effect of Lithofacies on Gas Storage Capacity of marine and continental Shales in the Sichuan Basin, China. *J. Nat. Gas Sci. Eng.* 36, 773–785. doi:10.1016/j.jngse.2016.11.024

Couch, E. L. (1971). Calculation of Paleosalinities from Boron and Clay Mineral Data1. *AAPG Bull.* 55, 1829–1837. doi:10.1306/819a3dac-16c5-11d7-8645000102c1865d

Feng, Y., Li, S., and Lu, Y. (2013). Sequence Stratigraphy and Architectural Variability in Late Eocene Lacustrine Strata of the Dongying Depression, Bohai Bay Basin, Eastern China. *Sediment. Geology.* 295, 1–26. doi:10.1016/j.sedgeo.2013.07.004

Guan, Y. Z. (1992). The Element, clay mineral and Depositional Environment in Horqin Sand Land. *J. Desert Res.* 12, 9–15.

Han, C., Jiang, Z., Han, M., Wu, M., and Lin, W. (2016). The Lithofacies and Reservoir Characteristics of the Upper Ordovician and Lower Silurian Black Shale in the Southern Sichuan Basin and its Periphery, China. *Mar. Pet. Geology.* 75, 181–191. doi:10.1016/j.marpetgeo.2016.04.014

He, J., Ding, W., Jiang, Z., Li, A., Wang, R., and Sun, Y. (2016). Logging Identification and Characteristic Analysis of the Lacustrine Organic-Rich Shale Lithofacies: A Case Study from the Es3L Shale in the Jiyang Depression, Bohai Bay Basin, Eastern China. *J. Pet. Sci. Eng.* 145. doi:10.1016/j.petrol.2016.05.017

Hickey, J. J., and Henk, B. (2007). Lithofacies Summary of the Mississippian Barnett Shale, Mitchell 2 T.P. Sims Well, Wise County, Texas. *Bulletin* 91, 437–443. doi:10.1306/12040606053

Li, P., Zhang, J., Rezaee, R., Dang, W., Tang, X., Nie, H., et al. (2021). Effect of Adsorbed Moisture on the Pore Size Distribution of marine-continental Transitional Shales: Insights from Lithofacies Differences and clay Swelling. *Appl. Clay Sci.* 201, 105926. doi:10.1016/j.clay.2020.105926

Liang, C., Zaixing, J., Yingchang, C., Jing, W., Yongshi, W., and Fang, H. (2017). Sedimentary Characteristics and Origin of Lacustrine Organic-Rich Shale in the Salinized Eocene Dongying Depression. *Geol. Soc. America Bull.* 130. doi:10.1130/b31584.1

Liu, H., Zhang, S., Song, G., Zhang, S., Hao, X., Xie, Z., et al. (2017). A Discussion on the Origin of Shale Reservoir Inter-laminar Fractures in the Shahejie Formation of Paleogene, Dongying Depression. *J. Earth Sci.* 28, 1064–1077. doi:10.1007/s12583-016-0946-3

Loucks, R. G., and Ruppel, S. C. (2007). Mississippian Barnett Shale: Lithofacies and Depositional Setting of a Deep-Water Shale-Gas Succession in the Fort Worth Basin, Texas. *Bulletin* 91, 579–601. doi:10.1306/11020606059

Ma, Y., Fan, M., Lu, Y., Liu, H., Hao, Y., Xie, Z., et al. (2016). Climate-driven Paleolimnological Change Controls Lacustrine Mudstone Depositional Process and Organic Matter Accumulation: Constraints from Lithofacies and Geochemical Studies in the Zhanhua Depression, Eastern China. *Int. J. Coal Geology.* 167, 103–118. doi:10.1016/j.coal.2016.09.014

Ma, Y., Fan, M., Lu, Y., Liu, H., Hao, Y., Xie, Z., et al. (2017). Middle Eocene Paleohydrology of the Dongying Depression in Eastern China from Sedimentological and Geochemical Signatures of Lacustrine Mudstone. *Palaeogeogr. Palaeoclimatol. Palaeoecol.* 479, 16–33. doi:10.1016/j.palaeo.2017.04.011

Maiti, S., Krishna Tiwari, R., and Kümpel, H.-J. (2007). Neural Network Modelling and Classification of Lithofacies Using Well Log Data: a Case Study from KTB Borehole Site. *Geophys. J. Int.* 169, 733–746. doi:10.1111/j.1365-246x.2007.03342.x

Peng, X. F., Wang, L. J., and Jiang, L. P. (2012). Geochemical Characteristics of the Lucaogou Formation Oil Shale in the southeastern Margin of the Junggar Basin and its Environmental Implications. *Bull. Mineralogy Pet. Geochem.* 31, 121–127.

Pepper, A. S., and Corvi, P. J. (1995). Simple Kinetic Models of Petroleum Formation. Part I: Oil and Gas Generation from Kerogen. *Mar. Pet. Geology.* 12, 291–319. doi:10.1016/0264-8172(95)98381-e

Su, S., Jiang, Z., Shan, X., Ning, C., Zhu, Y., Wang, X., et al. (2019). Effect of Lithofacies on Shale Reservoir and Hydrocarbon Bearing Capacity in the Shahejie Formation, Zhanhua Sag, Eastern China. *J. Pet. Sci. Eng.* 174, 1303–1308. doi:10.1016/j.petrol.2018.11.048

Tang, X., Jiang, Z., Huang, H., Jiang, S., Yang, L., Xiong, F., et al. (2016). Lithofacies Characteristics and its Effect on Gas Storage of the Silurian Longmaxi marine Shale in the Southeast Sichuan Basin, China. *J. Nat. Gas Sci. Eng.* 28, 338–346. doi:10.1016/j.jngse.2015.12.026

Walker, C. (1968). Evaluation of Boron as a Paleosalinity Indicator and its Application to Offshore Prospects. *Aapg Bull.* 52. doi:10.1306/5d25c45d-16c1-11d7-8645000102c1865d

Wang, Y., Wang, X., Song, G., Liu, H., Zhu, D., Ding, J., et al. (2016). Genetic Connection between Mud Shale Lithofacies and Shale Oil Enrichment in Jiyang Depression. *Bohai Bay Basin* 43, 696–704. doi:10.1016/s1876-3804(16)30091-x

Yang, C., Zhang, J., Tang, X., Ding, J., Zhao, Q., Dang, W., et al. (2017). Comparative Study on Micro-pore Structure of marine, Terrestrial, and Transitional Shales in Key Areas, China. *Int. J. Coal Geology.* 171, 76–92. doi:10.1016/j.coal.2016.12.001

Yang, Wan-qin., Jiang, You-lu., and Wang, Yong. (2015). Study on Shale Facies Sedimentary Environment of Lower Es3-Upper Es4 in Dongying Sag [J]. *J. China Univ. Petroleum(Edition Nat. Science)* 39 (4), 19–26.

Yang, Wanqin., Wang, Xuejun., and Zhang, Shun. (2018). Lake Paleoclimate Quantitative Recovery and its Effects on fine-grained Sedimentary : An Example from Es4s to Es3x in Dongying Sag [J]. *Pet. Geology. Recovery Efficiency* 25 (2), 29–35.

You, H., Cheng, R., and Liu, C. (2002). Review of Paleosalinity Recovering Methods [J]. World Geology. 21 (2), 111–117.

Zhang, G.-l., Chen, S.-y., Wang, H.-f., and Zhang, P.-f. (2009a). Sedimentary Characteristics and Lithofacies Paleogeography Evolution of Pero-Carboniferous System in Jiyang Depression. *J. China Univ. Pet. (Edition Nat. Science)* 33, 11–17.

Zhang, L., Liu, Q., Zhu, R., Li, Z., and Lu, X. (2009b). Source Rocks in Mesozoic-Cenozoic continental Rift Basins, east China: A Case from Dongying Depression, Bohai Bay Basin. *Org. Geochem.* 40, 229–242. doi:10.1016/j.orggeochem.2008.10.013

Zhu, R., Zhang, L., Zheng, L. I., Wang, R., Zhang, S., and Zhang, L. (2019). Evaluation of Shale Oil Resource Potential in continental Rift basin:A Case Study of Lower Es_3 Member in Dongying Sag. *Pet. Geology. Recovery Efficiency*.

Zong, G., Xiao, H., and Li, C. (1999). Evolution of Jiyang Depression and its Tectonic Implications. *Geol. J. China Universities* 5, 275–282.

Conflict of Interest: Author HL was employed by Shengli Oilfield Company of Sinopec.

The remaining authors declare that the research was conducted in the absence of any commercial or financial relationships that could be construed as a potential conflict of interest.

Publisher's Note: All claims expressed in this article are solely those of the authors and do not necessarily represent those of their affiliated organizations, or those of the publisher, the editors, and the reviewers. Any product that may be evaluated in this article, or claim that may be made by its manufacturer, is not guaranteed or endorsed by the publisher.